Journal of Hydraulic Engineering
Manuscript Draft

Manuscript Number: HYENG-7146

Title: A Pseudo-Transient Continuation-Based Finite Element Hydrodynamic Model for Dam and Levee Failure.

Article Type: Technical Note

Abstract: This technical note presents the development and application of a Pseudo-Transient Continuation-based flow model for the simulation of dam and levee failure. The unstructured, implicit, finite element model relies on computed residuals to automatically adjust the time step size. The result is an efficient and accurate prediction of both the speed and depth of shock waves as the dam-break flow passes over initially dry and wet land.

A Pseudo-Transient Continuation-Based Finite Element Hydrodynamic Model for Dam and Levee Failure

By Gaurav Savant[1], Tate O. McAlpin[2], Charlie Berger[3], Jennifer N. Tate[4]

Abstract: This technical note presents the development and application of a Pseudo-Transient Continuation-based flow model for the simulation of dam and levee failure. The unstructured, implicit, finite element model relies on computed residuals to automatically adjust the time step size. The result is an efficient and accurate prediction of both the speed and depth of shock waves as the dam-break flow passes over initially dry and wet land.

Introduction

Accurate and efficient numerical modeling of flows initiated by dam and levee failure (DLF) is a critical component of hydraulic as well as water resources engineering because of large increases in the flow volume routed through the water body, wave fronts as well as rapid flooding of the banks. Due to these several concurrent phenomenon DLF problems are particularly challenging when compared to other hydrodynamic flows such as flows forced through tides or river discharge/stage.

Modeling flows initiated by dam and levee failures (DLF), historically, has been computationally inefficient, particularly for finite-element based implicit hydrodynamic models (Turan and Wang 2007 and Sarma and Saikia 2006). This inefficiency can be attributed to uncertainty in the initial time step size and the number of iterations to be utilized during time stepping. This computational inefficiency has produced claims that implicit finite element hydrodynamic models are unsuitable for modeling rapidly expanding problems such as DLF., In fact this belief is widespread enough that scientific studies ,attempting to understand DLF problems numerically, do not even consider finite element based hydrodynamic methods worth the time and effort (Turan and Wang 2007). However, it stands to reason that improvement in the time-stepping algorithm could result in a more computationally efficient solution to the problem at hand.

[1] Research Water Resources Engineer, Dynamic Solutions LLC, Onsite Contractor Engineer Research and Development Center, US Army Corps of Engineer, Vicksburg, MS 39180, Gaurav.Savant@usace.army.mil.
[2] Research Physicist, Engineer Research and Development Center, US Army Corps of Engineers, Vicksburg, MS 39180, Tate.O.McAlpin@usace.army.mil.
[3] Research Hydraulic Engineer, Engineer Research and Development Center, US Army Corps of Engineers, Vicksburg, MS 39180, Charlie.Berger@usace.army.mil,
[4] Research Hydraulic Engineer, Engineer Research and Development Center, US Army Corps of Engineers, Vicksburg, MS 39180, Jennifer.N.Tate@usace.army.mil.

Time marching through a DLF problem is particularly time consuming because the initial iterate does not include complex features such as shocks. This is the particular area where Pseudo-Transient Continuation (PTC) can take advantage of the partial differential equation (PDE) structure and converge to a solution more efficiently.

PTC is a numerical technique for steady state computation of time dependent partial differential equations (Kelley and Keyes 1998). In general, PTC is a predictor-corrector technique for temporal integration in which the time step is increased or decreased as the objective of the convergence nears a solution or variation tolerance (Coffey et. al., 2002).

Pseudo Transient Continuation

Suppose we have a problem of the type

$$F(u) = 0 \tag{1}$$

where $\mathrm{F}:\mathrm{R}^{\mathrm{N}} \to \mathrm{R}^{\mathrm{N}}$ is continuous differentiable.

The Newton solution to this problem is

$$U_{+} = U_{c} + s \tag{2}$$

Where $s = F(u_c)/\left(-F'(u_c)\right)$, and $F'(u_c)$ is the Jacobian, subscript '+' indicates the new solution, and subscript 'c' indicates the solution at the present time.

If *F* is smooth and *s* is obtained using a direct solve, two outcomes are possible: 1) the solution might be bad, because the iterations are unbounded or the derivatives tend to singularity, or 2) the solution is satisfactory and the values obtained are real and physical. This implies that the problem will come to a solution or produce an error that is easy to detect. DLF problems are tough to solve because differential singularities have a high probability of occurring in the solution scheme, and the solution achieved might be non-physical. That is, outcome 1), above is common when trying to solve DLF problems.

Now, assume a boundary value problem of the type (Kelley at. al., 1998)

$$\frac{dm}{dt} = -F(m), \quad \text{where } m(0) = m_0. \tag{3}$$

For a DLF problem the PDE in the domain consists of:

1. nonlinearity
2. boundary conditions

3. spatial derivatives.

The purpose of solving the problem is to obtain a steady state solution such that

$$m^* = \lim_{t \to \infty} m(t) \tag{4}$$

where m^* is the steady state solution.

If we utilize a Newton type solver for this problem there are at least two distinct possibilities. There might be a shock in the system e.g. a flood wave moving, or the matrix might be stiff. There are a variety of numerical remedies to these possibilities such as setting the error tolerance to a very small value, or the utilization of a very small time step. These options will solve the problem but will require a large computational effort making the cost to benefits ratio extremely high so as to render the entire exercise fruitless. PTC is a mathematical technique designed to solve some of these problems.

PTC involves integrating equations of the type described in equation 3 to steady state by increasing the time step size. The implicit Euler representation of equation 3 is

$$m_+ = m_c + \Delta t F\left(m_+\right) \tag{5}$$

where subscript '+' indicates the new solution, and subscript 'c' indicates the solution at the present time.

The PTC representation for a single Newton iterate has been shown to be (Coffey et.al. 2002)

$$m_+ = m_c - \left(1/\Delta t + F'\left(m_c\right)\right)^{-1} F\left(m_c\right) \tag{6}$$

Or, in error terms

$$\left\| m_c - \left(I/\Delta t + F'\left(m_c\right)\right)^{-1} F\left(m_c\right) - m_+ \right\| \le \eta_c \tag{7}$$

$\| \ \|$ indicates the L_2 norm. For direct solvers or analytic Jacobians, the error η_c is exactly zero.

In a pure PTC mathematical solution the goal is to achieve steady state by utilizing large time steps determined based on error ratios. The purpose of PTC in DLF type applications is to provide the worst error after one Newton iterate; this error is by definition the worst error that will be encountered during time stepping if the problem is well posed.

DLF problems are not steady state problems, therefore the time step selection has to be conservative so as to resolve the transient temporal terms. Switched evolution relaxation (SER) (Mulder and van Leer 1985) is a numerical technique for auto-time step selection and is dependent on a previous time step, a previous residual, and the residual after one Newton iterate at the present time, yielding the time step

$$\Delta t_n = \min\left(\Delta t_{n-1}\left\|F\left(m_{n-1}\right)\right\| / \left\|F\left(m_n\right)\right\|, \Delta t_{\max}\right) \tag{8}$$

However, in order to restrain the time step size taken in DLF problems SER was modified to utilize the time step size and residual at time t = 0. This is necessary because during Dam/Levee failures the propagation of the flood wave is equally if not more important than the state of the wave at a much further time ' $t \to \infty$ ', and restraining the time step will ensure temporal accuracy of the solution. Therefore, the time step is restrained such that:

$$\Delta t_n = \min\left(\Delta t_0\left\|F\left(m_0\right)\right\| / \left\|F\left(m_n\right)\right\|, \Delta t_{\max}\right) \tag{9}$$

This ensures that the time step selected is always restrained by the error encountered during a single Newton iterate at t=0, and hence prevents the time step from growing rapidly and drifting of the solution.. In order to maintain stability the authors suggest specifying the initial time step (Δt_0) as the explicit time step. The maximum step size should be restrained as some factor (>1) of the explicit time step as well.

Two-Dimensional Shallow Water Model Description

The model utilized for this study is the two-dimensional (2D) shallow water module of the US Army Corps of Engineers' unstructured finite element model ADaptive Hydraulics (ADH). Information about ADH can be accessed via the internet at https://adh.usace.army.mil.

The 2D shallow water equations are obtained by vertically integrating the mass and momentum under the assumptions of incompressible flow and hydrostatic pressure. Assuming negligible free surface shear and negligible fluid pressure at the free surface the 2D shallow water equations are written as given as

$$\frac{\partial \boldsymbol{U}}{\partial t} + \frac{\partial \boldsymbol{F}}{\partial x} + \frac{\partial \boldsymbol{G}}{\partial y} + \boldsymbol{H} = 0 \tag{10}$$

where

$$\boldsymbol{U} = \begin{Bmatrix} h \\ uh \\ vh \end{Bmatrix} \tag{11}$$

$$\boldsymbol{F} = \begin{Bmatrix} uh \\ u^2h + \frac{1}{2}gh^2 - h\frac{\sigma_{xx}}{\rho} \\ uvh - h\frac{\sigma_{yx}}{\rho} \end{Bmatrix} \tag{12}$$

$$\boldsymbol{G} = \begin{Bmatrix} vh \\ uvh - h\frac{\sigma_{xy}}{\rho} \\ vh^2 + \frac{1}{2}gh^2 - h\frac{\sigma_{yy}}{\rho} \end{Bmatrix} \tag{13}$$

and

$$\boldsymbol{H} = \begin{Bmatrix} 0 \\ gh\frac{\partial z_b}{\partial x} + gh\frac{n^2 u\sqrt{u^2+v^2}}{h^{1/3}} \\ gh\frac{\partial z_b}{\partial y} + gh\frac{n^2 v\sqrt{u^2+v^2}}{h^{1/3}} \end{Bmatrix} \tag{14}$$

Here, ρ = fluid density, u = flow velocity in the x direction, v = flow velocity in the y direction, h = flow depth, g = gravitational acceleration, z_b = riverbed elevation, and n = Manning's roughness coefficient. The σ = Reynolds stresses due to turbulence, where the first subscript indicates the direction, and the second indicates the face on which the stress acts.

The equations are discretized using the finite element method in which u, v, and h are represented as linear polynomials on each element. The actual finite element scheme is not of particular importance in this paper. It is an SUPG scheme similar to that reported in Berger and Stockstill (1995). Approximate values of velocity and depth are interpolated within an element from the element's nodal values (Tate et. al. 2006).

Equation 10 is composed of two distinct terms, 1) a temporal term and 2) a spatial term. The change in the spatial term is an indication of the slope of the temporal term. Utilizing this fact, the residual in the spatial terms is calculated for one Newton iterate to ascertain the L_2 norm for use in equation 9.

The PTC and SER techniques described above were implemented into ADH.

Testing

Tests were conducted to compare the numerical results from the described 2D shallow water model with PTC and SER incorporated into ADH (PTC-SER-ADH) and baseline ADH (no PTC or SER). Two different flume experiments were evaluated. The tests also compared the computational time required for solution using PTC-SER modified ADH and ADH without the use of PTC-SER.

The first case is a straight sloping flume in which a dam is instantaneously removed, producing a surge wave over initially dry land. The second case is a flat flume with a straight reach connected to a 45^{o} bend reach. The straight flume case is a 1-D problem while the angled case is a 2-D problem.

All of the tests were performed on a personal computer with Intel Pentium 4 processor- 3.4GHz, and 4GB of random access memory.

Case 1: Straight Flume

The first test case is a comparison with a study conducted at the US Army Corps of Engineer Engineering Research and Development Center (USACE, 1960, 1961). The flume was 121.9 m in length and 1.2 m in width. The flume had a slope of 0.0015. The dam is situated 61 m into the flume. Water is pooled upstream of the dam to a depth of 0.3048 m at the dam face, and the flume section downstream of the dam is dry. Data from the numerical model and the experiment were compared at the locations indicated in Figure 1.

The numerical mesh consisted of 1,200 elements and 755 nodes. The numerical domain is closed and the upstream and downstream walls are impermeable. The Manning's *n* value for the run was set at 0.009. The initial time step and the maximum time step to be utilized in equation 9 were 0.09 and 0.25 seconds, respectively. The time step sizes were selected from considerations of stability, the initial time step size is the smallest step size with which the model was able to run and the largest step size was the largest step the model could take for temporal accuracy and still maintain stability.

Figures 2 through 7 show the test results of time history of the water depths for stations 160, 191, 200, 225, 275 and 345. These station numbers are the distance along the flume in feet as indicated in Figure 1. The time of arrival of the surge wave in the numerical model, PTC-SER-ADH as well as ADH, agrees well with the flume observations.

For stations 200 and 275, the numerical model predicted results drop off faster in slope than the flume near the end of the run compared to the initial part of the run when the flume and the predicted results fall at the same rate.

The biggest difference is seen at station 200. The model captures the drop off in the water level but under predicts the peak depth around 50 seconds into the run.

The downstream stations (225, 275 and 345) compare well but also have some points of difference from the physical results. Overall the numerical results are in close agreement with the observed data. At station 275 the flood wave (surge) arrives approximately 5 seconds prior to the observed surge. The greatest error in the simulated depth of approximately 9% occurs at station 345, but the surge arrives at the same time as the observed surge.

Case 2: 45 º Bend Flume

The second test case is a comparison with a study reported in Brufau and Garcia-Navarro (2000). The flume combines a square reservoir and a 45º bend initially wet channel (Figure 8). The reservoir and the bend will essentially experience 2-D flow. This is a particularly good test case because both the shock speed of the initial wave and the upstream moving hydraulic jump can be compared.

The reservoir is 2.44 m in length and 2.39 m in width, the length of the straight channel is 4.25 m, and the length of the angle section of the flume is 4.15 m. The width of both sections is 0.495 m. Initial water depth in the reservoir is 0.25 m and the channel has an initial depth of 0.01 m. The Manning's *n* value reported in the study for the flume bottom and the side walls were 0.0095 and 0.0195, respectively. The computational mesh consisted of 8,150 elements and 4,316 nodes. The initial and the maximum time step size for use with equation 9 were 0.009 and 0.25 sec, respectively.

Observations were made at 9 points inside the flume (Figure 9), however due to uncertainty in behavior of the downstream boundary comparisons are shown only for points P1, P2, P3, P4, P5, and P8 (Figures 10-15).

In general, the figures indicate good agreement between the ADH predicted and observed depths and shock speeds. Experimental data show high frequency oscillations which can not be captured by means of the 2D shallow water equations with the hydrostatic assumption. There are noticeable differences in the depth at the tail end of the simulations and it appears that the water is pooling instead of flowing out. This might be attributed to the treatment of the downstream boundary.

Stations P2 and P3 show excellent agreement between the observed wave reflected at the bend and the ADH predicted wave celerity and depth.

Comparison of PTC-SER-ADH with ADH

Comparison runs were conducted between ADH and ADH modified with PTC-SER to determine the efficiency of the PTC-SER-ADH model over the ADH model without utilizing PTC-SER. Computational times are shown for run parameters where the PTC-SER-ADH and ADH hydrodynamic results were the same. Tables 1 and 2 tabulate the results of these runs for test Case 1 and 2, respectively.

PTC-SER-ADH shows great improvements over the ADH model without PTC-SER. In Case 1, to obtain the same hydrodynamic results PTC-SER-ADH required approximately 80 % of the time required by ADH with similar time steps and the same number of iterations. For Case 2, the utilization of PTC-SER resulted in even greater time efficiency and required approximately 70% of the time required by a similar ADH run without PTC-SER. Case 2 is a more difficult problem to solve than Case 1 because Case 2 is essentially a 2D problem whereas Case 1 is 1D. This seems to indicate that the more complicated a problem the better PTC-SER-ADH performs in terms of time efficiency.

Conclusions

The US Army Corps of Engineers 2D hydrodynamic model, ADaptive Hydraulics (ADH) with Pseudo Transient Continuation (PTC) is being developed for application to the numerical simulation of dam failure/levee breach type of problems.

The numerical model was validated through comparisons with two separate studies involving dam failure in a flume setting. In general the model shows good agreement with the shock speeds and depths for surges over initially dry land (Case 1) and initially wet land (Case 2).

Run time comparisons between PTC-SER-ADH and ADH show that the incorporation of PTC-SER into ADH provides increased time efficiency of as much as 30% over ADH.

Acknowledgment

The experiments described and results presented in this paper were obtained through research sponsored by the US Army Corps of Engineers System Wide Water Resources Program (SWWRP). Permission was granted by the Chief of Engineers to publish this information.

References

Berger, R. C., and Stockstill, R. L. (1995). "Finite element model for high velocity channels." *Journal of Hydraulic Engineering*, 121(10), 710-716.

Brufau P. and Garcia-Navarro P. (2000). "Two-dimensional dam break flow simulation." *International Journal for Numerical Methods in Fluids*, 33, 35-57.

Coffey T. S., Kelley C. T., and Keyes, D. E.(2002). "Pseudo-Transient continuation and differential-algebraic equations." Submitted to *SIAM Journal of Scientific Computing*.

Kelley C. T. and Keyes D. E. (1998). "Convergence analysis of pseudo-transient continuation." *SIAM Journal of Numerical Analysis*, 35, 508-523.

Mulder, W. A., van Leer, B. (1985). "Experiments with implicit upwind methods for the Euler Equation." *Journal of Computational Physics*, 59, 232-246.

Sarma, A. P. and Saikia, D. S. (2006). "Dam break hydraulics in natural rivers". *World Environmental and Water Resources Congress, ASCE Conference Proceedings 200, 69(2006).*

Tate, J. N., Berger, R. C., and Stockstill, R. L. (2005). "Refinement indicator for mesh adaption in shallow-water modeling." *Journal of Hydraulic Engineering*, 132(8), 854-857.

Turan, B and Wang, K-H (2007). "Flood and Shock Waves simulation by using finite volume technique on unstructured meshes*." World Environmental and Water Resources Congress 2007*.

U.S. Army Engineer Waterways Experiment Station (1960). "Floods resulting from suddenly breached dams: Conditions of minimum resistance." Paper: 2-237, report 1.

U.S. Army Engineer Waterways Experiment Station (1961). "Floods resulting from suddenly breached dams: Conditions of maximum resistance." Paper: 2-374, report 2.

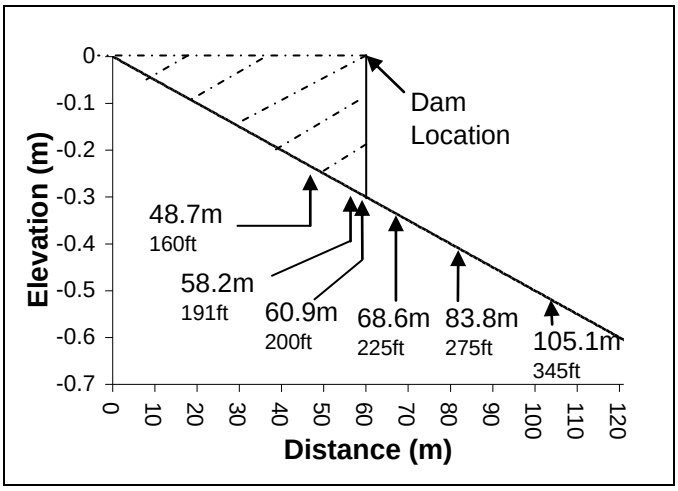

Figure 1: Layout of Straight Flume (elevation view) with observation stations (numbers under the metric locations indicate observation stations)

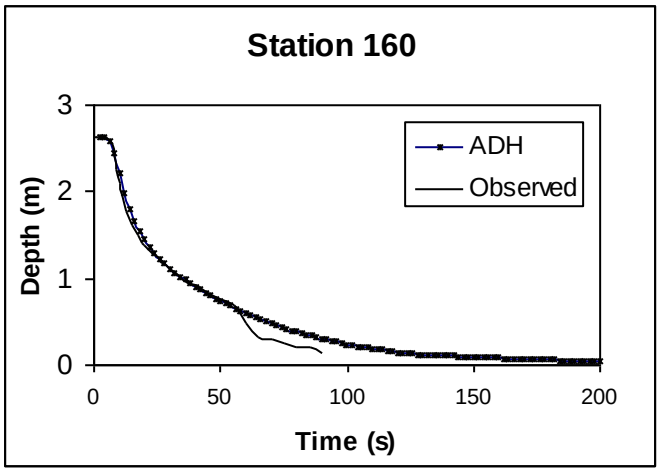

Figure 2: Depth Comparison for ADH and flume experiment, sta 160

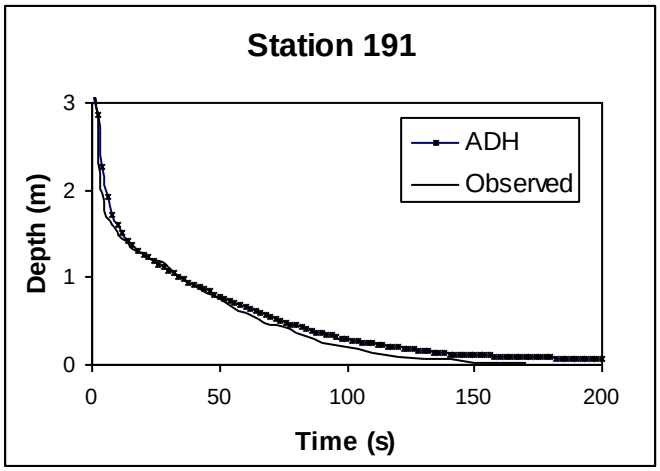

Figure3: Depth Comparison for ADH and flume experiment, sta 191

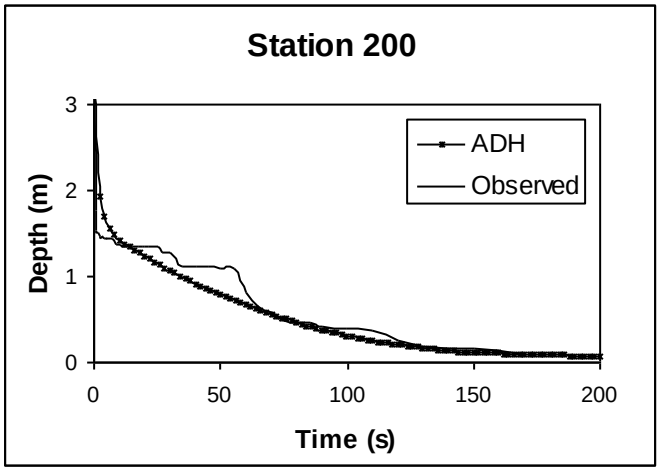

Figure 4: Depth Comparison for ADH and flume experiment, sta 200

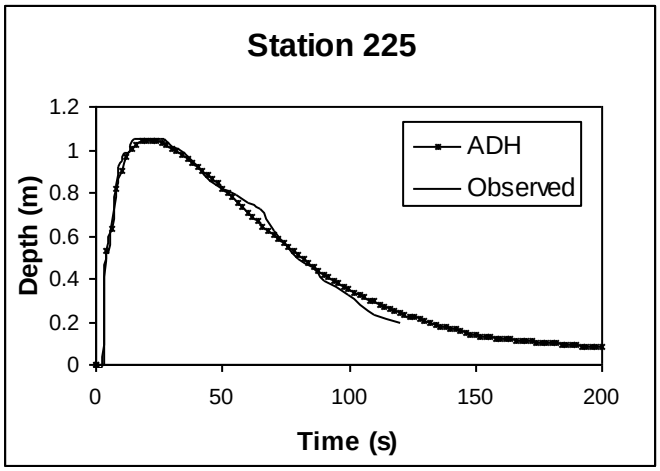

Figure 5: Depth Comparison for ADH and flume experiment, sta 225

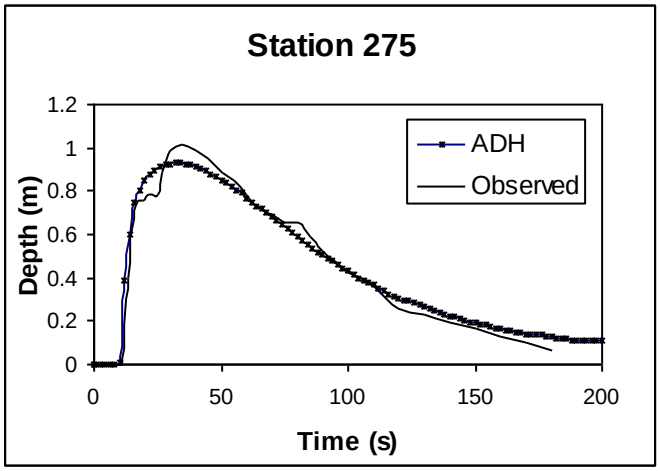

Figure 6: Depth Comparison for ADH and flume experiment, sta 275

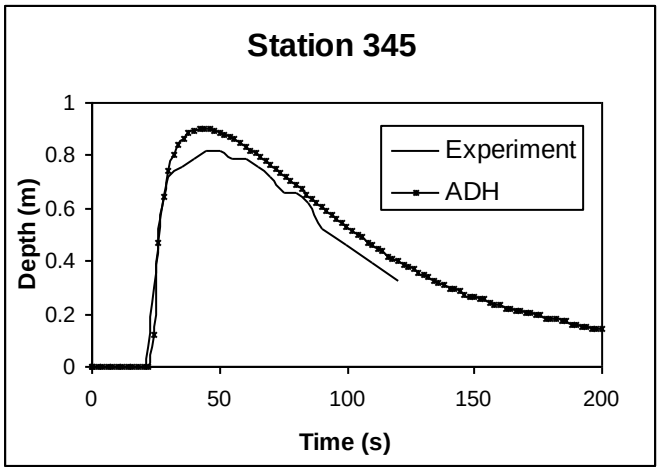

Figure 7: Depth Comparison for ADH and flume experiment, sta 345

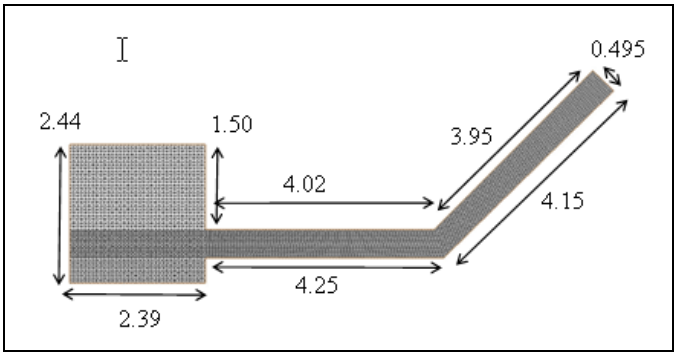

Figure 8: Numerical Test Flume (dimensions in meters)

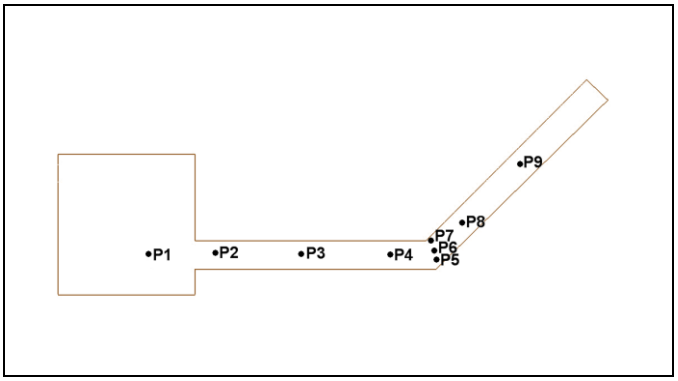

Figure 9: Observation Points

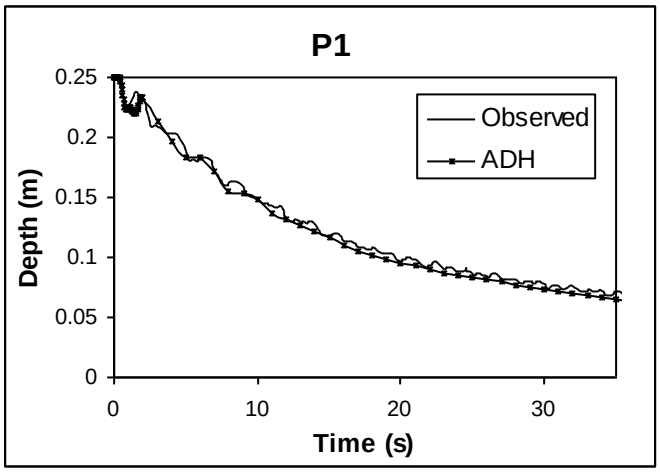

Figure 10: Depth Comparison for ADH and flume experiment, sta P1

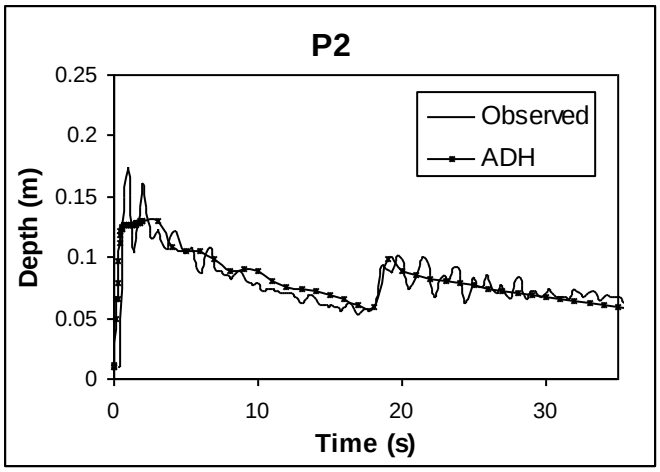

Figure 11: Depth Comparison for ADH and flume experiment, sta P2

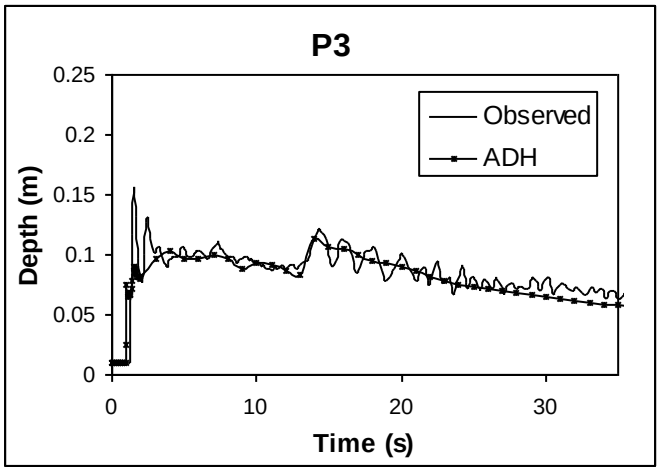

Figure 12: Depth Comparison for ADH and flume experiment, sta P3

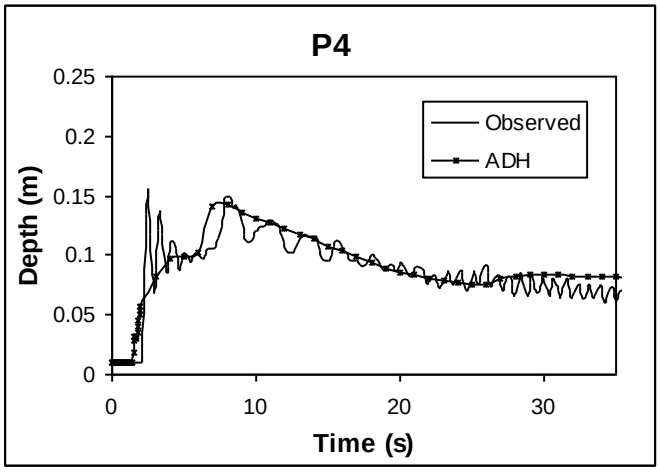

Figure 13: Depth comparison for ADH and flume experiment, sta P4

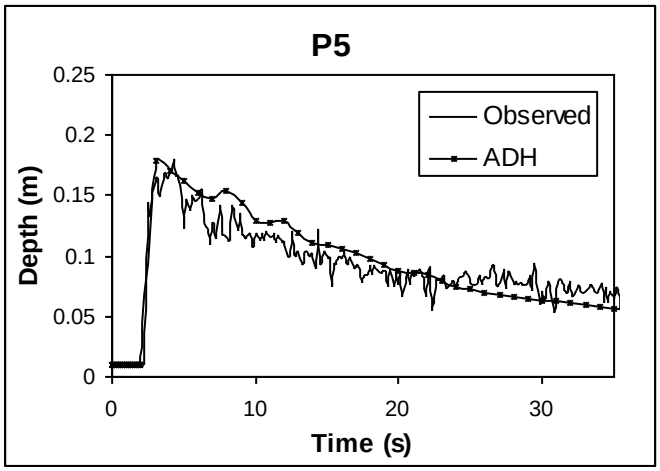

Figure 14: Depth comparison for ADH and flume experiment, sta P5

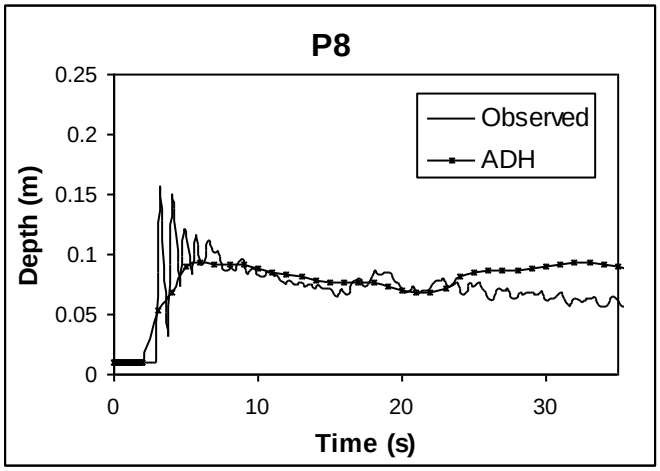

Figure 15: Depth Comparison for ADH and flume experiment, sta P8

Table 1: Case1- Model Time Comparison for ADH and PTC-SER-ADH

Model	ADH	ADH	PTC-SER-ADH
Number of Iterations	5	5	5
Initial Time Step (s)	0.09	5	0.09
Final Time Step (s)	0.5	5	0.5
Time to Completion (s)	374	418	300

Table 2: Case2- Model Time Comparison for ADH and PTC-SER-ADH

Model	ADH	ADH	PTC-SER-ADH
Number of Iterations	5	5	5
Initial Time Step (s)	0.009	5	0.009
Final Time Step (s)	0.5	5	0.25
Time to Completion (s)	582	1020	420

Sizing worksheet (.xls)

Click here to download Sizing worksheet (.xls): MSizingWebExcel (1).xls

ASCE Worksheet for Sizing Technical Papers & Notes

*****Please complete and save this form then email it with each manuscript submission.*****

Note: The worksheet is designed to automatically calculate the total number of printed pages when published in ASCE tw format.

Journal Name:	**Journal of Hydraulic Engineering**	**Manuscript # (if known):**	
Author Full Name:	ɾant, Tate O. McAlpin, Charlie Berger, Jenr	**Author Email:**	gaurav.savant@usac

The maximum length of a technical paper is 10,000 words and word-equivalents or 8 printed pages. A technical note should not exceed 3,500 v word-equivalents in length or 4 printed pages. Approximate the length by using the form below to calculate the total number of words in the tex it to the total number of word-equivalents of the figures and tables to obtain a grand total of words for the paper/note to fit ASCE format. Over must be approved by the editor; however, valuable overlength contributions are not intended to be discouraged by this procedure.

1. Estimating Length of Text

A. Fill in the four numbers (highlighted in green) in the column to the right to obtain the total length of text.

NOTE: Equations take up a lot of space. Most computer programs don't count the amount of space around display equations. Plan on counting 3 lines of text for every simple equation (single line) and 5 lines for every complicated equation (numerator and denominator).

Estimating Length of Text		
Count # of words in 3 lines of text:		54
Divided by 3		3
Average # of words per line		18
Count # of text lines per page		19
# of words per page		342.00
Count # of pages (don't add references & abstract)		16
Title & Abstract		500
Total # refs	10	242
Length of Text is		6214
		415
		6629
		6

2. Estimating Length of Tables

A. First count the longest line in each column across adding two characters between each column and one character between each word to obtain total characters.

1-column table = up to 60 characters wide	2-column table = 61 to 120 characters wide

B. Then count the number of text lines (include footnote & titles)

1-column table = up to 60 characters wide by:	**2-column table = 61 to 120 characters wide by:**
17 lines (or less) = 158 word equiv.	17 lines (or less) = 315 word equiv.
up to 34 lines = 315 word equiv.	up to 34 lines = 630 word equiv.
up to 51 lines = 473 word equiv.	up to 51 lines = 945 word equiv.
up to 68 text lines = 630 word equiv.	up to 68 text lines = 1260 word equiv.

C. Total Characters wide by Total Text lines = word equiv. as shown in the table above. **Add word equivalents** for each table in the column labeled "**Word Equivalents.**"

3. Estimating Length of Figures

A. First reduce the figures to final size for publication.

Figure type size can't be smaller than 6 point (2mm).

B. Use ruler and measure figure to fit 1 or 2 column wide format.

1-column fig. = up to 3.5 in.(88.9mm)	2-col. fig. = 3.5 to 7 in.(88.9 to 177.8 mm) wide

C. Then use a ruler to check the height of each figure (including title & caption).

1-column fig. = up to 3.5 in.(88.9mm) wide by:	**2-column fig. = 3.5 to 7 in.(88.9 to 177.8 mm) wide by:**
up to 2.5 in.(63.5mm) high = 158 word equiv.	up to 2.5 in.(63.5mm) high = 315 word equiv.
up to 5 in.(127mm) high = 315 word equiv.	up to 5 in.(127mm) high = 630 word equiv.
up to 7 in.(177.8mm) high = 473 word equiv.	up to 7 in.(177.8mm) high = 945 word equiv.
up to 9 in.(228.6mm) high = 630 word equiv.	up to 9 in.(228.6mm) high = 1260 word equiv.

D. Total Characters wide by Total Text lines = word equiv. as shown in the table above. **Add word equivalents** for each table in the column labeled **"Word Equivalents."**

Estimating Length of Tables &		
Tables	Word Equivalents	**Figures**
Table 1	158	Figure 1
2	158	2
3	0	3
4	0	4
5	0	5
6	0	6
7	0	7
8	0	8
9	0	9
10	0	10
11	0	11
12	0	12
13	0	13
14	0	14
15	0	15
Please double-up tables/figures if additional space is needed (ex. 20+21).		16
		17
		18
		19
		20 and 21

Total Tables/Figures:	2686	(word equivalents)
Total Words of Text:	6629	

Total words and word equivalents:		**9315**
	printed pages:	**8**

updated 1/16/03